Diffeomorphic Atlas Estimation using Kärcher Mean and Geodesic Shooting on Volumetric Images

François-Xavier Vialard[1]
http://www.doc.ic.ac.uk/~fvialard/
Laurent Risser[2]
http://laurent.risser.free.fr/
Darryl Holm[1]
http://www2.imperial.ac.uk/~dholm/
Daniel Rueckert[2]
http://www.doc.ic.ac.uk/~dr/

[1] Department of Mathematics
Imperial College London
London, UK

[2] Department of Computing
Imperial College London
London, UK

Abstract

In this paper, we propose a new algorithm to estimate diffeomorphic organ atlases out of 3D medical images. More precisely, we explore the feasibility of Kärcher means by using *large deformations by diffeomorphisms* (LDDMM). This framework preserves organs topology and has interesting properties to quantitatively describe their anatomical variability. We also use a new registration algorithm based on an optimal control method to satisfy the geodesicity of the deformations at any step of the optimisation process. Initial tangent vectors to the shapes, which are used to compute the Kärcher mean, are therefore estimated accurately. Our methodology is tested on different groups of 3D images representing organs with a large anatomical variability.

1 Introduction

In the field of *Computational Anatomy*, the Riemannian point of view on shape spaces has provided efficient tools to perform of powerful statistical methods [3, 4]. The driving motivation of this work is to quantify, on real 3D images, the anatomical variability of biological shape populations, with a particular attention to the topology preservation of the organs. We therefore study a topology preserving method for averaging biological shapes. For biomedical data like 3D cerebral images for instance, preserving the structures topology is a key challenge when registering or averaging images. Diffeomorphic techniques are then of high interest since they can encode large deformations while preserving the shape topology. Defining an average shape in a diffeomorphic framework has been addressed in several works, using deterministic [1] or Bayesian approaches [9]. Mixed methods using intensity voxel averaging and diffeomorphic registration have also been developed in [6]. The averaging method of [6] does not however preserve the shape topology, since it mixes two averaging strategies, which are the Kärcher mean [3, 7], *i.e.* intrinsic mean on Riemannian

manifold, and an extrinsic mean as explained in [3]. In this work, we study the strategy of [4, 11] to compute the Kärcher mean on images using the framework of *large deformations by diffeomorphisms* (LDDMM) [2, 5, 8]. Compared with [4, 11], the novelty of our study is that we use this strategy on segmented 3D medical images requiring large deformations. We also use a new geodesic shooting algorithm which ensures geodesic transformations at each registration iteration and only at convergence like the standard LDDMM algorithm of [2]. Since the convergence is often truncated to keep the computational burden reasonable, this strategy is more suitable than [2] to compute Kärcher means.

2 Optimal control for geodesic shooting

We consider two scalar images I and J defined on a domain Ω. Their registration consists in the minimization of the functional $\mathscr{E}(u) \doteq \frac{1}{2}\int_0^1 \|u_t\|_V^2\, dt + \|I\circ\phi_{0,1}^{-1} - J\|_{L^2}^2$, where $u \in L^2([0,1],V)$ is a time-dependent velocity field and the space V is usually a Reproducing Kernel Hilbert Space of smooth vector fields defined on Ω. The deformation $\phi_{0,1}$ is generated by the ODE $\frac{d}{ds}\phi_{t,s} = v_s\circ\phi_{t,s}$, where $\phi_{t,t} = Id$. The minimization of the functional $\mathscr{E}$ can be carried over the geodesic flow, which leads to the minimization of

$$\mathscr{S}(P_0) = \frac{\lambda}{2}\langle \nabla I_0 P_0, K\star\nabla I_0 P_0\rangle_{L^2} + \frac{1}{2}\|I_1 - J\|_{L^2}^2\,, \tag{1}$$

subject to the shooting system

$$\begin{cases} \partial_t I_t + \nabla I_t\cdot v_t = 0\,,\\ \partial_t P_t + \nabla\cdot(P_t v_t) = 0\,,\\ v_t + K\star\nabla I_t P_t = 0\,, \end{cases} \tag{2}$$

with initial condition P_0 for the initial momentum. In order to compute the gradient of (1), we follow an optimal control approach: We introduce a time-dependent Lagrange multiplier to constrain the paths to be geodesics. The gradient of $\mathscr{S}$ is given by: $\nabla_{P_0}\mathscr{S} = -\hat{P}_t + \lambda\nabla I_t\cdot K\star(P_0\nabla I_0)$ where $\hat{P}_0$ is given by the solution of the following PDE solved backward in time:

$$\begin{cases} \partial_t \hat{I}_t + \nabla\cdot(v_t\hat{I}_t) + \nabla\cdot(P_t\hat{v}_t) = 0\,,\\ \partial_t \hat{P}_t + v_t\cdot\nabla\hat{P}_t - \nabla I_t\cdot\hat{v}_t = 0\,,\\ \hat{v}_t + K\star(\hat{I}_t\nabla I_t - P_t\nabla\hat{P}_t) = 0\,, \end{cases} \tag{3}$$

subject to the initial conditions $\hat{I}_1 = J - I_1$, $\hat{P}_1 = 0$ and P_t, I_t are the solution of the shooting system (2) for the initial conditions I_0, P_0. Existence of the geodesic flow (2) and the solutions to the adjoint equations (3) can be proven, provided that the source and target images are sufficiently smooth, namely H^2. The algorithm to compute the gradient is divided into two steps: First, solving the shooting system (2) forward from the initial conditions I_0, P_0; second, solving backward the adjoint equations (3).

3 Kärcher mean

We use the methodology of [3, 11] to define the average of a group of images having the same topology. Given a group of imaged shapes $I^1,\dots,I^n$ and a Riemannian metric d on the

images, an average can be defined as a minimizer of

$$\mathscr{M}(I) = \frac{1}{2n}\sum_{k=1}^{n} d(I,I^k)^2\,. \tag{4}$$

Remark that the uniqueness is not guaranteed in general. However, in finite dimensions it can be proven that if the group of data lies in a sufficiently small neighborhood, there exists a unique minimizer to (4). Since the matching between the registered images is not exact, we also approximate (4) by $\mathscr{M}(I) \approx \frac{1}{2n}\sum_{k=1}^{n} d(I,I_1^k)^2$, where I_1^k is the result of the shooting equations for the initial condition $P_0 = P_0^k$ and P_0^k is a minimizer of the matching functional (1) for $J = I^k$. In this case, the squared distance is given $\langle P_0, K\star P_0\rangle_{L^2}$ and the gradient of $\mathscr{M}$ is given by

$$\nabla\mathscr{M}(I) = -\frac{1}{n}\sum_{k=1}^{n} K\star\nabla I P_0^k\,, \tag{5}$$

where P_0^k is the initial momentum matching I on I^k via the shooting system (2). In particular, at an average shape I^{mean}, the gradient of $\mathscr{M}$ vanishes. In this situation, the gradient is given by (5). The intrinsic mean is given by a gradient descent procedure. We first initialize $T^0 = I^1$, $\varepsilon > 0$ and $\alpha > 0$. We then repeat until convergence (1) Register T^i on each I^k for $k \in [1,n]$ with geodesic shooting and extract P_0^k the corresponding initial momentum. (2) Compute $P^{mean} = \frac{\alpha}{n}\sum_{k=1}^{n} P_0^k$. (3) Compute I_1 from (3) with initial conditions $I_0 = T^i$ and $P_0 = P^{mean}$ and update $T^{i+1} = I_1$. The convergence of this algorithm can be assessed via the norm of the momentum P_{mean}.

4 Results

4.1 Experimental data and parameters

We test here the ability of our algorithm to estimate average shapes for different groups of 3D imaged organs: (1) Eight segmented hippocampal images randomly selected out of the healthy controls of the Alzheimer's Disease Neuroimaging Initiative (ADNI) study. (2) eight 3D MR brain scans acquired, with a spatial resolution of 0.85mm, on several preterm infants between 29 and 31 weeks of gestational age. Probabilistic segmentation of the brain gray matter were performed on each subject using [10]. (3) eight other 3D MR brain scans pre-treated with the same protocol, but acquired on preterm infants between 37 and 39 weeks of gestational age. As shown in Fig. 1, these three image groups have different levels of complexity. We denote in all tests R^n, $n \in [1,\cdots,N]$ the reference images and A_i^n the average image estimate after i iterations, where $A_0^n = R^n$. We finally define the kernels K by using the multi-kernel technique of [12] incorporate a multi-scale information in the the metrics. For the brains, the kernel K is defined as the sum of two isotropic Gaussian kernels of standard deviation 25mm and 1.5mm. When registering the hippocampuses, we however use a simple Gaussian kernel K with a standard deviation of 1mm.

4.2 Convergence for different initial guesses

We now validate our methodology by measuring the influence of the initial guess. For a set of reference shapes and an initial guess, the algorithm converges to an optimal average shape. However, there is no uniqueness of the optimised shape for different initial guesses. We then

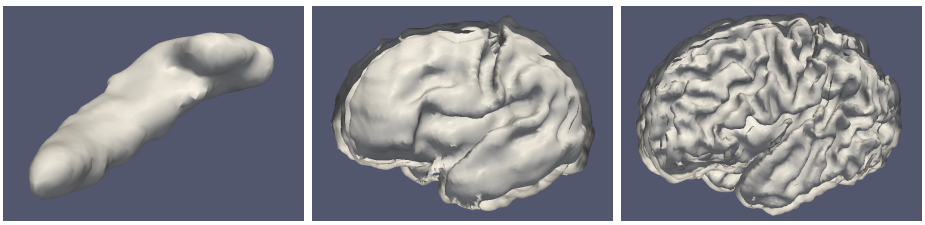

Figure 1: Isosurface of typical segmented 3D MR images from which the average shapes are estimated. **(From left to right)** Isosurface of a hippocampus and inner face of cortical surfaces out of two pre-term baby acquired at 30 and 38 weeks of gestational age.

measure here the similarity of the average shape estimates using different initial guesses. In each distinguished reference image dataset R^n, $n \in [1,\cdots,N]$, we pick up 3 different initial guesses and perform average shape estimations. In Fig. 2, we show the evolution of the 3D images of 30 weeks old cortexes in a 2D slice during the 3 first iterations. In order to quantify the similarity of the different images, we also measure $S(A_i^1,\cdots,A_i^3) = \frac{1}{8}\sum_{m=1}^{3}\sum_{p=1}^{3} SSD(A_i^m,A_i^p)$, where $SSD(.,.)$ is the sum of squared differences between two images. If S is null, then the average estimates are all the same and the higher this value, the more different are the images. Results are given in Fig. 2 .

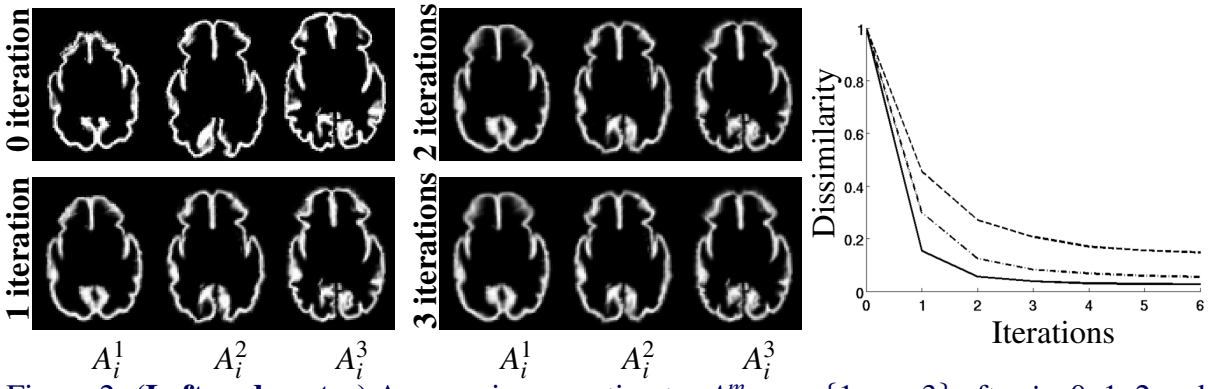

Figure 2: **(Left and centre)** Average image estimates A_i^m, $m \in \{1,\cdots,3\}$ after i =0, 1, 2 and 3 iterations, where m represents the identifier of the initial guess. Here the the evolution of the 3D shapes of 30 weeks old cortexes are shown in a 2D slice. **(Right)** Normalised similarity of the average estimates A_i^m for different initial guesses m in function of the iteration number i. Similarities $S(A_i^1,\cdots,A_i^3)$ are shown for the hippocampuses (continuous line), the 30 weeks brains (semi dashed line) and the 38 weeks brains (dashed line).

In all the considered cases, the average estimates are increasingly similar. Interestingly, the influence of the initial guess is very weak after only one iteration for the hippocampuses and a few iterations for the 30 weeks old brains as shown Fig. 2. The convergence is however slower for the more complex 38 years old brain. We can indeed observe in Fig. 2 that while about 85% of the differences are lost in one iteration for the hippocampuses and two iterations for the 30 weeks old brains, five iterations are needed for the 38 weeks old brains for a similar result. This number of iterations remains however limited regarding the differences in the initial guesses. The proposed methodology therefore appears efficient to estimate average shapes but requires an increasingly number of iterations according to the complexity of the reference shapes.

5 Conclusion

In this work, we have successfully explored the Kärcher mean strategy of [4, 11] in a diffeomorphic setting, to estimate average shapes on 3D medical images requiring large deformations. To this end, our main contribution is to use a new geodesic shooting technique within the LDDMM framework. The averaging strategy therefore preserves the shape topology even for organs having a large variability and it does not require intensity averaging. We have also shown that the algorithm computes good estimates of the averaged shapes in very few iterations for shapes requiring small deformations and a limited number of iterations for more complex shapes. The immediate perspective of this work is to estimate temporal atlases of the early cortical growth. Other potential directions consist in performing descriptive and inferential statistics on 3D and 3+t shape populations.

References

[1] B. Avants and J. Gee. Shape averaging with diffeomorphic flows for atlas creation. In *Proceedings of IEEE ISBI*, 2004.

[2] M F Beg, M I Miller, A Trouvé, and L Younes. Computing large deformation metric mappings via geodesic flow of diffeomorphisms. *IJCV*, 61:139–157, 2005.

[3] P. T. Fletcher, C. Lu, M. Pizer, and S. Joshi. Principal geodesic analysis for the study of nonlinear statistics of shape. *IEEE Trans. Med. Imaging*, pages 995–1005, 2004.

[4] P. T. Fletcher, S. Venkatasubramanian, and S. Joshi. Robust statistics on riemannian manifolds via the geometric median. In *Proceedings of CVPR*, pages 1–8, 2008.

[5] J. Glaunès, M. Vaillant, and M. I. Miller. Landmark matching via large deformation diffeomorphisms on the sphere. *J. Math. Imag. Vis.*, 20:179–200, 2004.

[6] S. Joshi, Brad Davis, Matthieu Jomier, and Guido Gerig. Unbiased diffeomorphic atlas construction for computational anatomy. *NeuroImage*, 23:151–160, 2004.

[7] H. Karcher. Riemannian center of mass and mollifier smoothing. *Comm. Pure Appl. Math.*, 30(5):509–541, 1977. ISSN 0010-3640.

[8] P. Lorenzen, B. Davis, and S. Joshi. Unbiased atlas formation via large deformations metric mapping. In *MICCAI 2005*, volume 8, pages 411–418, 2005.

[9] J. Ma, M. I. Miller, A. Trouvé, and L. Younes. Bayesian template estimation in computational anatomy. *Neuroimage*, 42(1):252–261, 2008.

[10] M Murgasova, P Aljabar, L Srinivasan, S J Counsell, V Doria, A Serag, I S Gousias, J P Boardman, M A Rutherford, A D Edwards, J V Hajnal, and D Rueckert. A dynamic 4D probabilistic atlas of the developing brain. *NeuroImage*, 54(4):275–63, 2011.

[11] Xavier Pennec. Intrinsic statistics on riemannian manifolds: Basic tools for geometric measurements. *Journal of Mathematical Imaging and Vision*, 25:127–154, 2006.

[12] L Risser, F X Vialard, Wolz R, M. Murgasova, D D Holm, and D Rueckert. Simultaneous Multiscale Registration using Large Deformation Diffeomorphic Metric Mapping. *IEEE Trans. Med. Imaging*, 2011.